

Chloroplast/thylakoid-rich material

Sutcharit, Pomarat; Wattanakul, Jutarat; Price, Ruth; di Bari, Vincenzo; Gould, Joanne; Yakubov, Gleb; Wolf, Bettina; Gray, David A.

DOI:

[10.1016/j.foodres.2023.112472](https://doi.org/10.1016/j.foodres.2023.112472)

License:

Creative Commons: Attribution-NonCommercial-NoDerivs (CC BY-NC-ND)

Document Version

Peer reviewed version

Citation for published version (Harvard):

Sutcharit, P, Wattanakul, J, Price, R, di Bari, V, Gould, J, Yakubov, G, Wolf, B & Gray, DA 2023, 'Chloroplast/thylakoid-rich material: a possible alternative to the chemically synthesised flow enhancer polyglycerol polyricinoleate in oil-based systems', *Food Research International*.
<https://doi.org/10.1016/j.foodres.2023.112472>

[Link to publication on Research at Birmingham portal](#)

General rights

Unless a licence is specified above, all rights (including copyright and moral rights) in this document are retained by the authors and/or the copyright holders. The express permission of the copyright holder must be obtained for any use of this material other than for purposes permitted by law.

- Users may freely distribute the URL that is used to identify this publication.
- Users may download and/or print one copy of the publication from the University of Birmingham research portal for the purpose of private study or non-commercial research.
- User may use extracts from the document in line with the concept of 'fair dealing' under the Copyright, Designs and Patents Act 1988 (?)
- Users may not further distribute the material nor use it for the purposes of commercial gain.

Where a licence is displayed above, please note the terms and conditions of the licence govern your use of this document.

When citing, please reference the published version.

Take down policy

While the University of Birmingham exercises care and attention in making items available there are rare occasions when an item has been uploaded in error or has been deemed to be commercially or otherwise sensitive.

If you believe that this is the case for this document, please contact UBIRA@lists.bham.ac.uk providing details and we will remove access to the work immediately and investigate.

1 **Chloroplast/Thylakoid-rich Material: A Possible Alternative to the Chemically Synthesised Flow**
2 **Enhancer Polyglycerol Polyricinoleate in Oil-Based Systems**

3 Poramat SUTCHARIT^a (poramat.sucharit@nottingham.ac.uk), Jutarat WATTANAKUL^{a, b}
4 (jutarat.wattanakul@nottingham.ac.uk), Ruth PRICE^a (ruth.price@nottingham.ac.uk), Vincenzo Di
5 Bari^a (vincenzo.dibari@nottingham.ac.uk), Joanne GOULD^a (joanne.gould@nottingham.ac.uk), Gleb
6 YAKUBOV^a (gleb.yakubov@nottingham.ac.uk), Bettina WOLF^c (B.wolf@bham.ac.uk), David A. GRAY^{a*}
7 (David.gray@nottingham.ac.uk)

8

9 ^a Division of Food, Nutrition and Dietetics, School of Biosciences, University of Nottingham, Sutton
10 Bonington Campus, Loughborough LE12 5RD, United Kingdom.

11 ^b Department of Food Sciences and Technology, Faculty of Home Economics Technology, Rajamangala
12 University of Technology Krungthep, Bangkok, 10120, Thailand.

13 ^c School of Chemical Engineering, University of Birmingham, Edgbaston Campus, Birmingham B15 2TT,
14 United Kingdom.

15 *Corresponding author's telephone: +44 (0) 115 951 6147

16

17

18

19

20

21

22

23

24

25 **Abstract**

26 Chloroplasts are abundant organelles in a diverse range of plant materials; they are
27 predominantly composed of multicomponent thylakoid membranes which are lipid and protein rich.
28 Intact or unravelled thylakoid membranes should, in principle, have interfacial activity, but little has
29 been published on their activity in oil-in-water systems, and nothing on their performance on an oil
30 continuous system. In this work different physical methods were used to produce a range of
31 chloroplast/thylakoid suspensions with varying degrees of membrane integrity. Transmission electron
32 microscopy revealed that pressure homogenisation led to the greatest extent of membrane and
33 organelle disruption compared to less energy intensive preparation methods The ability of the derived
34 materials to modulate the flow behaviour of a chocolate model system (65% (w/w) sugar/ sunflower
35 oil (natural amphiphiles removed) suspension) was investigated by acquiring rheological parameters.
36 All chloroplast/thylakoid preparations reduced yield stress, apparent viscosity, tangent flow point and
37 cross over point in a concentration-dependent fashion, although not as significantly as polyglycerol
38 polyricinoleate applied at a commercially relevant concentration in the same chocolate model system.
39 Confocal laser scanning microscopy confirmed presence of the alternative flow enhancer material at
40 the sugar surfaces. This research reveals that low-energy processing methods that do not extensively
41 disrupt thylakoid membranes are applicable to generating materials with marked capacity to affect
42 the flow behaviour of a chocolate model system. In conclusion, chloroplast/thylakoid materials hold
43 strong potential as natural alternatives to synthetic rheology modifiers for lipid-based systems such
44 as PGPR.

45

46 **Key words:** Chocolate; Rheology; Casson model; Emulsifier; Yield stress; Apparent Viscosity;
47 chloroplast; thylakoid membranes

48

49 **Abbreviations**

50 η_{40} : Apparent Viscosity at 40 seconds⁻¹ (Pa s)

51 BCRF: Burst Chloroplast-rich Fraction (wet sample)

52 B-CRF: Burst Chloroplast-rich Fraction (dried powder sample)

53 COP: Cross Over Point (Pa)

54 η_c : Casson Viscosity (Pa s)

55 σ_c : Casson Yield Stress (Pa)

56 CP: Combined Pellet, P1 and P2 (wet sample)

57 DP: Diluted Pellet (wet sample)

58 DP-CRF: Diluted Pellet Chloroplast-rich Fraction (dried powder sample)

59 J-Method: Juicing Method

60 P1: Pellet 1 (First Centrifugation) (wet sample)

61 P2: Pellet 2 (Second Centrifugation) (wet sample)

62 P-CRF: Pellet Chloroplast-rich Fraction (dried powder sample)

63 PGPR: Polyglycerol Polyricinoleate

64 S-CRF: Rhodamine B Stained Chloroplast-rich Fraction (dried powder sample)

65 $\dot{\gamma}$: Shear Rate (s⁻¹)

- 66 σ : Shear Stress (Pa)
- 67 SJ: Spinach Juice
- 68 s/o: Sugar-in-Oil Suspension
- 69 SN1: Supernatant 1 (First Centrifugation)
- 70 SN2: Supernatant 2 (Second Centrifugation)
- 71 TFP: Tangent Flow Point (Pa)
- 72 WBSJ: Water Blended Spinach Juice (wet sample)
- 73 WBTRF: Water Blended Thylakoid-rich Fraction (wet sample)
- 74 WB-Method: Water Blending Method
- 75 τ_5 : Yield Stress at 5 seconds⁻¹ (Pa)
- 76

77 **1. Introduction**

78 Chocolate is one of the most popular and highly consumed confections products worldwide.
79 Originating from Central and South America, roasted and ground cacao beans (*Theobroma cacao* L.)
80 have been used in various confectionery products such as chocolate bars and drinks. Chocolate
81 consists mainly of ground, roasted cocoa nibs, cocoa butter and milled sugar (Beckett, 2009). The flow
82 behaviour of molten chocolate is highly dependent on manufacturing steps, such as mixing, refining,
83 conching, tempering and moulding (Shafi, Reshi, Aiman, & Bashir, 2018), and formulation such as
84 solids particle size and lipid fraction (Afoakwa, Paterson, & Fowler, 2007; Beckett, 2009). Frequently
85 formulations also contain emulsifiers to tune the rheological properties of molten chocolate for
86 moulding or enrobing processes (Afoakwa, 2016). Parameters such yield stress (σ), apparent viscosity
87 (η_a), tangent flow point (TFP) and cross over point (COP) are commonly used in practice to quantify
88 the flow behaviour of chocolate (Afoakwa, Paterson, Fowler, & Vieira, 2009; Beckett, 2009; De Graef,
89 Depypere, Minnaert, & Dewettinck, 2011; Peker, Suna, Tamer, & Copur, 2013; Servais, Ranc, &
90 Roberts, 2003).

91 In chocolate the hydrophilic part of an emulsifier molecule associates with the sugar particle
92 surfaces while the hydrophobic part extends into the continuous cocoa butter phase. One of the most
93 common emulsifiers used in confectionery products to control yield stress (σ) is polyglycerol
94 polyricinoleate (PGPR, Food label - E476) (Schantz & Rohm, 2005; Sözeri Atik, Bölük, Toker, Palabiyik,
95 & Konar, 2020). PGPR is a chemical compound obtained through acid esterification of castor oil in the
96 presence of polyglycerol (Wilson, Van Schie, & Howes, 1998). Although PGPR has been deemed as safe
97 by the Joint FAO/WHO Expert Committee on Food Additives (FECFA), the Scientific Committee of Food
98 (SCF) (Ministers, 2002) and 'generally recognised as safe' (GRAS) by the Food and Drugs Administration
99 (FDA) as well as deemed safe following a recent re-evaluation by the European Food Safety Authority
100 (EFSA Panel on Food Additives Nutrient Sources added to Food et al., 2017), restrictions on quantities
101 used in confectionery products are still being carefully monitored: 0.3% (w/w) in the US; 0.5% (w/w)
102 in Canada, Australia, New Zealand and the European Union (EU) (Quest International, 1997).

103 Nevertheless, consumers increasingly prefer clean-label products (Osborn, 2015) which drives the
104 confectionery industry to look for a natural alternative to the synthetic PGPR, i.e., a natural amphiphile
105 that is effective in controlling the yield stress of chocolate.

106 Chloroplasts, organelles ubiquitous in the biosphere that convert sunlight energy into
107 chemical energy (in the form of sugar), are an abundant source of interfacial-active galactolipids. With
108 a diameter between 3 – 10 μm , chloroplasts contain three different membrane systems: the outer-
109 and inner-envelope membranes, and the thylakoid membrane (Block, Dorne, Joyard, & Douce, 1983).
110 Enriched with macro- and micro-nutrients (Mohamed A. Gedi et al., 2017; M. A. Gedi et al., 2019;
111 Syamila, Gedi, Briars, Ayed, & Gray, 2019; Torcello-Gomez et al., 2019; Jutarat Wattanakul et al., 2019),
112 chloroplasts were reported to possess interfacial-active properties which have been shown to retard
113 fat digestion, (Albertsson et al., 2007; Ostbring et al., 2018) and stabilise oil-in-water emulsions
114 (Rayner, Emek, Gustafssona, Albertsson, & Albertsson, 2011; Rayner, Ljusberg, et al., 2011; Tenorio,
115 de Jong, Nikiforidis, Boom, & van der Goot, 2017). In a separate study, the extracted chloroplast lipids
116 enhanced the flow properties in a moderately concentrated sugar-in-oil-suspension (Mohamad, Gray,
117 & Wolf, 2020). The objective of this work was to assess the ability of intact chloroplast membranes, a
118 lesser refined natural system than extracted lipids avoiding the use of organic solvents (e.g., hexane,
119 chloroform and/or methanol) during preparation, to replace PGPR in future chocolate formulations.
120 In contrast to Mohamad et al. (2020), a highly concentrated sugar-in-oil (s/o) suspension (65% (w/w)
121 sugar, equivalent to 53% (v/v)), was recently developed for the comparative assessment of
122 commercial PGPR samples by Price, Gray, Watson, Vieira, and Wolf (2022); this model was used as the
123 chocolate model system. The naturally present amphiphiles in the oil phase were removed prior to
124 preparing the suspension to ensure the rheological parameter values could be related to the action of
125 the chloroplast/thylakoid systems alone. Such systems were prepared from spinach leaf, an easy-
126 accessible green leaf tissue system applied in previous related work (Mohamed A. Gedi et al., 2017;
127 Mohamad et al., 2020; Jutarat Wattanakul et al., 2022) using juicing and blending methods. It was

128 hypothesised that the loss of chloroplast integrity would be accompanied by an increase in de-stacked,
129 liberated thylakoid membranes which in turn would increase the interfacial activity of the material
130 per unit mass and ultimately reduce the yield stress in the s/o suspension. Based on microscopy and
131 particle size analysis a subset of chloroplast/thylakoid systems of varying degrees of integrity was
132 selected and applied in the suspensions. Their rheological properties were then compared to those of
133 suspension containing PGPR as interfacial-active additive and the results interpreted in conjunction
134 with micrographs acquired on the suspensions.

135

136 **2. Materials and Methods**

137 **2.1 Materials**

138 A total of 9 kg of spinach leaves (*Spinacia oleracea* L.) was purchased from a local store (Tesco,
139 Nottingham, United Kingdom) and immediately stored at 4°C (Polysec Coldrooms Ltd, Worcester,
140 United Kingdom) until use. Sunflower oil (*Helianthus annus* L.) was also purchased from a local store
141 (Sainsburys, Nottingham, United Kingdom) and stored at room temperature in the dark. Polyglycerol
142 polyricinoleate (PGPR), Palsgaard 4150 and Grindsted 90, was gifted by Palsgaard A/S (Juelsminde,
143 Denmark) and Danisco A/S (Copenhagen, Denmark), respectively. EM grade glutaraldehyde,
144 cocadylate buffer, osmium tetroxide, uranyl acetate, ethanol, propylene oxide, resin solutions, sodium
145 hydroxide and lead citrate were kindly provided by the Nanoscale and Microscale Research Centre at
146 the University of Nottingham (Nottingham, United Kingdom). Magnesium silicate (Florisil®),
147 rhodamine B, isopropanol and n-heptane were of HPLC grade and purchased directly from Sigma-
148 Aldrich (Darmstadt, Germany) and Thermo Fisher Scientific (Waltham, Massachusetts, United States).

149

150 **2.2 Methods**

151 **2.2.1 Preparation of Chloroplast Fractions via Juicing Method**

152 A juicing method was applied to prepare a chloroplast-rich pellet from spinach leaves, see also
153 Fig. 1. The spinach leaves were weighed, washed thoroughly with tap water, and divided into batches
154 of approximately 1 kg. Before proceeding to the juicing process, the leaves were partially dried using
155 a domestic 'salad spinner'. Leaves were juiced using a vegetable juicer (Angel Juicer 7500 Angel Juicer
156 Co., Ltd, Busan, South Korea), filtered (75 μ m) and centrifuged (Beckman J2-21, Beckman Coulter,
157 London, United Kingdom) (17,700 g, 10 minutes, 4°C) to obtain a chloroplast-rich pellet (Torcello-
158 Gomez et al., 2019). Spinach juice (SJ) was used as the control for chloroplast native state while the
159 centrifugation step was repeated twice to obtain supernatant samples (SN1, SN2), and pellet samples
160 (P1, P2).

161 One lot of pellet samples P1 and P2 was combined, referred to as CP or combined pellet
162 sample, and further processed as follows. CP (40 g) was transferred to a conical flask with 1 litre of
163 ultra-pure water (1:25 ratio) and thoroughly mixed with a magnetic stirrer (RCT digital, IKA-Werke,
164 Staufen, Germany) in the dark (600 rpm, 2 hours, 4°C). The diluted pellet (DP) was then homogenised
165 at 100 MPa (1,000 bar, 1 passage) using a high-pressure homogeniser (GEA Niro Soavi high-pressure
166 homogeniser, NS1001L2K, GEA, Düsseldorf, Germany). The pre-homogenised diluted pellet (DP) and
167 post-homogenised juice, termed burst chloroplast-rich fraction (BCRF), were collected, packed in a
168 vacuum sealed bags and stored at -20°C until use.

169

170 **2.2.2 Preparation of Thylakoid Fraction via Water Blending**

171 As an alternative to the juicing method, a water blending method adapted from literature
172 (Ostbring et al., 2018; Rayner, Emek, et al., 2011; Rayner, Ljusberg, et al., 2011) was applied, see also
173 Fig. 2. To 100 g of spinach leaves, 200 g of ultra-pure water (18.2 M Ω cm Milli-Q Direct water, Merck,
174 Darmstadt, Germany) was added (1:2 ratio), homogenised at full power using a blender (Kenwood
175 BLX510, United Kingdom) for 5 minutes, filtered (75 μ m) to obtain water blended spinach juice (WBSJ)

176 and centrifuged (6,400 g, 10 minutes, 4°C). The pellet was collected, diluted at 1:2 ratio with ultra-
177 pure water, thoroughly vortex and centrifuged (17,700 g, 15 minutes, 4°C) to obtain water blended
178 thylakoid-rich fraction (WBTRF) as the pellet at the bottom of the centrifuge tube. The filtered water
179 blended spinach juice (WBSJ) and pellet (WBTRF) were collected, packed in vacuum sealed bag and
180 store at -20°C until use.

181

182 **2.2.3 Lipid Extraction**

183 The process of total lipid extraction was performed following the protocol outlined by Folch
184 et al. (1957) and Bligh and Dyer (1959) with minor adjustments. To 0.1 g of the freeze-dried sample,
185 1.2 ml of 2:1 chloroform to methanol solution (CHCl₃: MeOH) was added and vortex (1 min). Prior to
186 centrifugation (3,000 rpm, 10 mins, 4°C), 0.9% sodium chloride (0.6 ml) was added and vortex for 1
187 minute. The lower phase (lipid extract) was collected along with an addition of 1.2 ml 2:1 CHCl₃:
188 MeOH, vortex (1 min) and centrifuged (3,000 rpm, 10 mins, 4°C). The extraction process was repeated
189 for three times. The accumulated lipid extracts then get centrifuged (3,000 rpm, 10 mins, 4°C),
190 extracted, filtered (0.45 µm, 13 mm) into a tared glass bijoux bottle and dried using nitrogen gas.

191

192 **2.2.4 Total Chlorophyll Analysis**

193 Dried lipid extracts were dissolved with acetone (1 ml), vortex (1 min) and perform further 2-
194 step serial dilution with acetone (1:250, 1:1,000, 1:2,000, 1:10,000) until the absorbance values fall
195 within the range of 0.1 – 1.0A. The total chlorophyll a (*Chl a*) and b (*Chl b*) pigment was measured
196 using UV-Vis Spectrophotometer (Genesys 10S, Thermo Fisher Scientific, Waltham, Massachusetts, 57
197 United States) at 662 and 645 nm respectively (Gedi et al., 2017, Torcello-Gomez et al., 2019). The
198 concentration of *Chl a* and *b* was calculated using equations (Eq. 3.1 and Eq. 3.2) suggested earlier by

199 Lichtenthaler (2001). The total chlorophyll content is calculated as the sum of both *Chl a* and *b* (Eq.
200 3.3).

$$201 \quad \text{Chl } a \text{ } (\mu\text{g/g}) = (11.24 \times A_{661.6}) - (2.04 \times A_{644.8}) \quad (\text{Eq. 3.1})$$

$$202 \quad \text{Chl } b \text{ } (\mu\text{g/g}) = (20.31 \times A_{644.8}) - (4.19 \times A_{661.6}) \quad (\text{Eq. 3.2})$$

$$203 \quad \text{Total Chlorophyll Content} = \text{Chl } a + \text{Chl } b \quad (\text{Eq. 3.3})$$

204

205 **2.2.5 Galactolipids Analysis**

206 The analysis of galactolipids (monogalactosyldiacylglycerol (MGDG) and
207 digalactosyldiacylglycerol (DGDG)) was performed using the high-performance thin layer
208 chromatography (HPTLC) technique.

209 To the dried lipid extracts, 1 ml of 2:1 chloroform to methanol solution (CHCl₃: MeOH) was
210 added. Both samples and standards were transferred to the same silica gel thin layer chromatography
211 (TLC) plate (Merck, Darmstadt, Germany) using the Hamilton syringe (Merck, Darmstadt, Germany)
212 and Linomat 5 (Camag, Muttenz, Switzerland). The injection setting was set to 1 µl (5 bars) and
213 repeated to reach the desired concentration. The plates were developed in a twin-trough chamber
214 (Camag, Muttenz, Switzerland) using the mobile phase (47.5: 10: 1.25, chloroform: methanol: water,
215 v/v/v) for 10 mins prior to drying in the fume hood (10 mins). Plate derivatization was performed using
216 Chromatogram Immersion Device 3 (Camag, Muttenz, Switzerland). In this experiment, thymol
217 solution is used to selectively stain the galactolipids (MGDG & DGDG) avoiding the interference that
218 may occur during the densitometric analysis by the HPTLC.

219 The thymol solution is prepared as follows. To 1 g of thymol, 190 ml of ethanol was added
220 following with a slow addition of 10 ml of sulphuric acid (96%) – the ice water bath was used to control
221 and avoid rapid exothermic reactions. After the derivatization, the plate was left to dry in the fume

222 hood (10 mins) and oven heated for 10 minutes at 110°C before the densitometric analysis. The
223 quantitative analysis of HPTLC (densitometric analysis) was perform using TLC Visualiser 2 (Camag,
224 Muttenz, Switzerland) and VisionCATs software (Camag, Muttenz, Switzerland). Image acquisition of
225 TLC plates were obtained under white light, 64 254 and 366 nm respectively. The determination of
226 galactolipids was calculated using the standard curve plotted from the MGDG and DGDG standards.

227

228 **2.2.6 Particle Size Analysis**

229 A Horiba Partica LA-960 Laser Scattering Particle Size Distribution Analyzer (Kyoto, Japan)
230 equipped with a tempax glass flow cell (Kyoto, Japan) was used to analyse the particle size distribution
231 of the chloroplast/thylakoid preparations. Every measurement was performed with two light sources
232 (405 and 650 nm) and the scattering patterns analysed following the Mie theory, utilising the
233 equipment's software. Triplicate measurements were carried out with agitation, circulation and the
234 transmission settings at level 2, 5 and between 70 – 95%, respectively. Relevant statistical analyses
235 were carried out as detailed later on.

236

237 **2.2.7 Microstructure Analyses of Prepared Chloroplast/Thylakoid Preparations**

238 **2.2.7.1 Light Microscopy**

239 Light micrographs were acquired with a transmitted light microscope (Nikon Eclipse Ci,
240 Shinagawa, Tokyo, Japan) to validate the light scattering particle size data and understand whether
241 the chloroplasts were intact or broken. All light micrographs were taken using phase contrast and a
242 40X objective lens. Based on 3 images and a total of 15 chloroplast structures per sample, chloroplast
243 particle size was estimated utilising image analysis software Fiji (Schindelin et al., 2012).

244

245 **2.2.7.2 Transmission Electron Microscopy**

246 Fresh chloroplast/thylakoid preparations were fixed with 3% EM grade glutaraldehyde in 0.1M
247 cacodylate buffer and stored overnight at 4°C. Washing steps (2 changes, 0.1M cacodylate buffer, 5
248 minutes) were performed and the preparations stored in 0.1M cacodylate buffer (1 ml, 4°C, dark)
249 before post-tissue-fixation with 1% osmium tetroxide in 0.1M cacodylate buffer (2 hours, room
250 temperature). Samples were then washed (2 changes, distilled water, 10 minutes), stained en bloc
251 (1% aqueous uranyl acetate, overnight, 4°C, dark), washed (3 changes, distilled water, 5 minutes) and
252 dehydrated with 50%, 70%, 90% (2 x 10 minute for each) and 100% ethanol (3 x 15 minutes),
253 respectively. To further remove water from the samples, propylene oxide (100%) was added (3
254 changes, 15 minutes, room temperature) followed by the addition of propylene oxide : resin (24 g TLV
255 Resin, 26 g TLV Hardener VH2) solution at 3:1 ratio (1 hour, room temperature) and 1:1 ratio
256 (overnight with lids off, room temperature), respectively. A pure resin preparation (TAAB Low
257 Viscosity Resin – hard recipe) was then added (2 changes, 1 hour) before embedding in the oven at
258 70°C for 48 hours. Samples were then sectioned with a diamond knife at 90 nm thick using a Leica EM
259 UC6 (Leica Biosystems, Wetzlar, Germany), placed on a 200-mesh carbon support copper grid and
260 stained with lead citrate. Grids were analysed using a Tecnai Bio-TWIN T12 Biotwin transmission
261 electron microscope (TEM) (FEI Company, Eindhoven, The Netherlands) at an accelerated voltage of
262 100 kV. Images were captured using a MegaView SIS camera at X9900 magnification.

263

264 **2.2.8 Sugar-in-oil Suspensions Preparation and Analyses**

265 **2.2.8.1 Preparation of Sugar-in-Oil Suspensions**

266 The first step of preparing the sugar-in-oil (s/o) suspensions involved the removal of naturally
267 present interfacial-active components in the continuous oil phase material, i.e., sunflower oil. The
268 sunflower oil was chosen for this experiment to create a simplified chocolate model making it easier

269 to interpret the effect of added complex chloroplast material. Moreover, various studies have also
270 used the sunflower oil as a continuous phase in s/o suspension to test the impact of different
271 emulsifiers (Manasi et al., 2019; Price et al., 2022). The oil was treated with 4% (w/w) magnesium
272 silicate (Florisil®) at 600 rpm for 30 minutes followed by centrifugation (2,700 g, 30 minutes, 20°C) to
273 remove the Florisil®. The treated oil, referred to simply as oil or sunflower oil in the following, was
274 stored in an amber glass bottle at 5°C in the dark until use. The icing sugar was also pre-treated by
275 drying in a vacuum oven at 60°C for 24 hours and stored in an air-tight container until use. The particle
276 size distribution of the dried icing sugar is provided in Appendix Fig. A.1 ($d_{4,3}$: $35.6 \pm 2.3 \mu\text{m}$).

277 The chloroplast samples chosen for incorporation into the s/o suspension included CP, DP and
278 BCRF. These materials were prepared as described earlier followed by freezing at -80°C for 24 h
279 (Denley, Massachusetts, United States), freeze-drying (Edwards, Burgess Hill, England) for 7 days,
280 grinding using a granite pestle and mortar, sieving (106 μm), vacuum-packaging and storage at -20°C
281 until use. Freeze-dried CP, DP and BCRF material is in the following referred to as P-CRF (pellet
282 chloroplast-rich fraction), DP-CRF (diluted pellet chloroplast-rich fraction) and B-CRF (burst
283 chloroplast-rich fraction).

284 The s/o suspensions were then prepared as follows. 75 g of purified sunflower oil was added
285 to a beaker containing dried chloroplast material (P-CRF, DP-CRF or B-CRF) (at the appropriate level
286 for the final suspension to contain 0.5, 1.0 or 2.0% w/w of this material) and stirred at 600 rpm for 1
287 h in the dark. The stirrer was removed, 75 g of dried icing sugar mixed in using a spatula followed by
288 using a high shear mixer (Silverson mixer L5 series) (8,000 rpm, 4 minutes, on ice). To simulate the
289 amount of particles in chocolate (65 – 75% w/w) (Afoakwa et al., 2007), the samples were centrifuged
290 (2,700 g, 10 minutes, 20°C), and the appropriate amount of oil supernatant removed to obtain a 65%
291 (w/w) (equivalent to 53%, v/v) sugar-in-oil suspension. PGPR stabilised suspensions were prepared
292 following the same protocol, replacing the chloroplast material with PGPR 4150 and G90 (0.1, 0.2 or
293 0.4% w/w in the final suspension).

294

295 **2.2.8.2 Rheological measurements**

296 Rheological measurements were performed using a stress-controlled rheometer (Physica
297 MCR 301, Anton Paar, Graz, Austria) equipped with a serrated cup and bob geometry (CC27, Anton
298 Paar, Graz, Austria). All measurements were performed in triplicate for each sample at a constant
299 temperature of 20°C. Unidirectional measurements were set up to follow a ramp-down protocol
300 (1,000 Pa to 0.01 Pa) (Price et al., 2022) and oscillatory measurements to follow a ramp-up protocol
301 (0.01 Pa to 100 Pa) at the constant angular frequency (ω) of 10 rad/s. For both types of measurements
302 10 logarithmically spaced data points were recorded per decade of stress, with each stress value
303 applied for 10 s prior to data capture.

304 The data from the unidirectional stress controlled (τ versus $\dot{\gamma}$) measurements was analysed
305 using RheoCompass software (Anton Paar, Frazm, Austria). The Casson model (Eq. 1) was used to
306 describe the flow behaviour of the model chocolate system.

$$307 \sigma^{0.5} = \sigma_c^{0.5} + (\eta_c \dot{\gamma})^{0.5} \quad (\text{Eq. 1})$$

308 σ and $\dot{\gamma}$ is shear stress and shear rate, σ_c and η_c indicates the Casson yield point and Casson
309 viscosity, respectively (Rao, 2014). In addition, the data were used to determine apparent viscosity at
310 40 s^{-1} (η_{40}) and shear stress at 5 s^{-1} (τ_5) taken to represent the yield stress (σ) (Servais et al., 2003).
311 For sake of clarity, τ_5 will be referred to as the “shear stress value at 5 s^{-1} (τ_5)”. In additional, the cross
312 over point (COP) and tangent flow point (TFP) were determined from the oscillatory measurements,
313 more specifically the dependency of the storage (G') and loss moduli (G'') on oscillatory stress. The
314 determination of both COP and TFP was found to be system specific and is described in detail when
315 introducing the results.

316

317 **2.2.8.3 Confocal Microscopy**

318 Filtered (75 μm) spinach juice (Section 2.2.1) was stained with rhodamine B (0.01 g/L) and
319 stirred at 600 rpm, 1 hour at room temperature. The objective of this staining is to stain the protein
320 components on the chloroplast and thylakoid structures (integral and peripheral membrane proteins)
321 prior to centrifugation. The sample was then centrifuged (17,700 g, 10 minutes, 4°C), frozen (24 hours,
322 -80°C) (Denley, Massachusetts, United States), freeze-dried (7 days) (Edwards, Burgess Hill, England),
323 ground and sieved (106 μm) to obtain stained chloroplast-rich fraction (S-CRF). The stained powder
324 was then vacuum-packed and stored at -20°C until a suspension sample was prepared containing this
325 powder. The suspension was prepared as described in 2.2.7.1 containing 1.0% S-CRF and the reduced
326 sugar level of 50% to facilitate imaging. A small sample of the suspension was dropped onto a slide
327 and gently spread out to maximise the clarity of microstructure. A Zeiss LSM 880 laser confocal
328 scanning microscope (Carl Zeiss AG, Oberkochen, Germany) installed with a red channel laser (561
329 nm) was used to image the microstructure. With the peak region selected for each slide, multiple
330 images were taken with a X63 objective lens and z-planes thicknesses of 0.5 and 0.2 μm .

331

332 **2.2.9 Statistical Analysis**

333 All measurements were conducted in triplicate measurements and the sample mean (\bar{x}),
334 standard deviation (SD) and standard error (SE) calculated. Using IBM SPSS Statistic 25, the Student t-
335 test was performed at $p \leq 0.05$ significant level or 95% confidence limit for every data set.

336

337 **3. Results and Discussion**

338 **3.1. Microstructure of Chloroplast/thylakoid materials**

339 An overview of the microstructures found in the various chloroplast/thylakoid materials,
340 prepared as summarised in Fig. 1 and 2, is provided in Fig. 3. As expected, the TEM micrograph from
341 the spinach juice shows a chloroplast structure with visible starch granules, mitochondria,
342 plastoglobules, and stacks of thylakoid membranes called grana (10 – 20 membrane layers) (Fig. 3, SJ).
343 According to Shimoni, Rav-Hon, Ohad, Brumfeld, and Reich (2005) and Wayne (2019), grana have a
344 diameter and thickness of approximately 0.3 and 0.2 - 0.6 μm , respectively. The grana and lamellae
345 structures of the thylakoid membrane can be clearly observed not only in the micrograph taken on SJ
346 but also those taken for in P1 and P2. By contrast, the images for SN1 and SN2 show rounded, vesicle-
347 shaped membrane structures that might have formed from disrupted chloroplasts. Although P1, P2
348 and WBTRF were all pellet samples, some degree of thylakoid membrane disruption (untangling of the
349 stacks) can be observed in the micrograph taken on WBTRF. On the other hand, the micrograph for
350 DP shows an unravelled membrane structure whilst the one for BCRF shows a completely
351 disintegrated membrane system. The latter is undoubtedly due to the high energy input during high
352 pressure homogenisation.

353 Particle size data of different chloroplast materials are shown in Fig. 4. A trimodal distribution
354 was observed for most samples. For instance, filtered SJ (Fig. 4, A) showed minor peaks at 0.2 and
355 101.5 μm , and a major peak at 4.5 μm . The major particle size fraction accounted for 80.0% of the
356 whole population and minor fractions for 4.0 and 16.0%, respectively. The major peak of 4.5 μm
357 compares well to data reported in literature as Möbius described in 1920 (Staehein, 1986) that an
358 intact chloroplast is approximately 3 – 10 μm in diameter. Here, the value was confirmed by estimating
359 the particle diameter from image analysis, with values of 4.4 ± 0.2 , 4.2 ± 0.3 and 5.2 ± 0.2 μm found
360 for CP, BCRF and WBTRF samples, respectively.

361 CP was obtained by centrifugation and the particle size distribution (Fig. 4) indicates a major
362 peak at 5.9 μm (96.2%) and a minor peak at 101.5 μm (3.8%). These values can be attributed to intact
363 chloroplast structures and the presence of debris/cell wall fragments and evidence that the

364 centrifugation step has successfully isolated intact chloroplasts. The particle size distributions of WBSJ
365 (peak values of 0.2 (~4%), 4.5 (~80%) and 101.5 μm (~16%)) and WBTRF (peak values of 3.9 (~79%)
366 and 59 μm (~21%)) closely resemble the distributions for SJ, DP and CP. However, the TEM
367 micrographs (Fig. 3) reveal a more dispersed membrane system for DP compared to WBSJ and WBTRF.
368 Following high pressure homogenisation (BCRF), the particle size distribution has not unexpectedly
369 shifted to smaller particle sizes with a major peak at 0.2 (~71%) and a minor yet pronounced peak at
370 2.0 μm (~29%). The microstructures shown in the corresponding TEM micrograph (Fig. 3, BCRF)
371 support the conclusion that high pressure homogenisation has disintegrated the chloroplast
372 membrane structure. Clearly, applying the range of processes considered in this work, summarised in
373 Fig. 1 and 2, allowed to manufacture chloroplast materials with different degrees of integrity.

374 From Fig. 3 and 4 it can also be seen that the membrane microstructures in the
375 chloroplast/thylakoid samples P1, DP and BCRF were distinctly different, including condensed,
376 untangled and disintegrated membranes, respectively. The microstructure of P2 material closely
377 resembled that of P1 and, thus, they were combined into one overall pellet sample (CP). As a
378 consequence, CP, DP and BCRF were chosen as the materials to be tested in the chocolate model
379 system (65% s/o suspension). All three samples were subjected to freeze-drying. After freeze-drying,
380 CP, DP and BCRF, will be referred to as P-CRF, DP-CRF and B-CRF, respectively. To measure the
381 efficiency of these CMMs' interfacial-active properties, they were tested in the chocolate model
382 system, in comparison to two commercial PGPR samples (PGPR 4150 and G90). Using the method
383 outlined earlier by Lichtenthaler (2001), the total chlorophyll analysis (Chl a and b) was performed.
384 The result indicates that P, DP and B-CRF contain similar amount of Chl ranging from approximately
385 42 – 48 mg/g DW. Upon applying the chloroplast material in the chocolate model system, depending
386 on the amount of CRF added, the concentration of Chl could varies between 0.021% (in 0.5% w/w
387 sample) to 0.084% (in 2.0% w/w sample).

388

389 3.2. Rheological characteristics

390 The Casson yield point (σ_c), the shear stress at 5 s^{-1} (τ_5), the apparent viscosity (η_{40}), the cross
391 over point (COP) and the tangent flow point (TFP) values determined for the s/o suspensions
392 containing P-CRF, DP-CRF, B-CRF, PGPR 4150, PGRP G90 or no added flow enhancer (control sample)
393 are reported in the Appendix Table A.1. The flow consistency index (η_c) (Chhabra, 1999) (also referred
394 to as viscosity consistency by Pratumwal et al. (2017)) obtained from fitting the Casson model to the
395 experimental data is shown in the Appendix Fig. B.2.

396 In the literature, multiple models and methods have been used to quantify the yield behaviour
397 of confectionery products (Afoakwa et al., 2009; Rao, 2014). The Casson yield stress, σ_c , is probably
398 the (still) most widely-used yield parameter in the confectionery industry (Rao, 2014). Applying the
399 Casson model to experimental data, initially not necessarily acquired in a prescribed manner, has been
400 the standard method approved by the International Confectionery Association (ICA) in 1973. In an
401 update, the use of pre-shear (5 s^{-1} , ≥ 5 mins) and up and down flow curves ($2 - 50 \text{ s}^{-1}$) to create the
402 experimental data for model fitting has been recommended (ICA Method 46) together with a more
403 complex rheological model (Eischen & Windhab, 2002) based on the Windhab equation (Windhab,
404 1993) and a shear rate correction (Eischen & Windhab, 2002). Nonetheless, the Casson model (Casson,
405 1959) is still widely used by many researchers (Cahyani et al., 2019; Kumbár, Nedomová, Ondrušíková,
406 & Polcar, 2018) and remains the model of choice for determining the yield stress of chocolate by the
407 National Confectioners Association (NCA) in the United States (formerly Chocolate Manufacturers
408 Association (CMA)) (Baker, Brown, & Anantheswaran, 2006).

409 The flow point (FP) describes the onset of flow dominated shear deformation. For the s/o
410 suspension systems it was found that determining the FP using oscillatory rheometry (FP_{osc}) is case
411 specific, meaning that the FP_{osc} determination procedure may require a degree of adjustment for
412 different samples. Initially, the suspension containing 0.4% PGPR 4150 was considered. At low
413 oscillatory stress this suspension displayed elastic dominated behaviour where $G' > G''$. With

414 increasing oscillatory stress, the system passed through a cross over point ($G' = G''$) and at higher
415 stresses viscous dominated behaviour where $G'' > G'$ was exhibited (Fig. 5). For this particular system,
416 two characteristic points can be determined: the tangent flow point and the cross over point. The
417 tangent flow point (TFP) is the crossing of the plateau modulus (i.e., G' Plateau) and the tangent of the
418 decay part of the oscillatory curve (i.e., slope tangent). Technically, it is possible to use the G'' curve
419 to determine another TFP, but this is not widely applied in literature (Dinkgreve, Paredes, Denn, &
420 Bonn, 2016; Malvern Instruments Limited, 2012). The cross over point (COP) is determined as the
421 value of the oscillatory stress where $G' = G''$, which marks the transition from elastic to viscous
422 dominated deformation. The G' Plateau was plotted using the data points in the region of linear
423 viscoelasticity (i.e., LVE), a range of tests which was carried out without destroying the sample's
424 structure. On the other hands, the slope tangent was plotted using the decay part of the collected G'
425 data. Both of these tangent lines can be use together to approximate the point of phase transition in
426 the sample. For the suspension with the higher amount of PGPR 4150 (0.6%), it can be seen that the
427 value for the Casson yield stress is almost negligible (Appendix Table A.1). However, a TFP could still
428 be determined although a COP does not exist since viscous dominated behaviour ($G'' > G'$) prevailed
429 throughout the range of oscillatory stresses applied. Yet another type of behaviour was observed for
430 the 0% PGPR sample, a discontinuity point. For stress values below the discontinuity point, the
431 sample's LVE behaviour was elastic dominated, whilst for oscillatory stresses above the discontinuity
432 point onset of flow was observed ($G'' > G'$). In such case, the TFP and COP points cannot be
433 distinguished and both coincide with the discontinuity point, which was taken as the flow point for
434 this type of system (Fig. 5).

435 Fig. 6 illustrates the flow curves for the formulated s/o suspensions across the range of
436 emulsifier systems and concentration applied, including the control sample (no emulsifier added). For
437 all samples, it was possible to identify a region of the flow curve that can be described as a high shear
438 plateau where the change in viscosity with shear stress is negligible. With decreasing shear stress, the

439 systems approached the yield point that sees a steep rise of the viscosity values. Fig. 6A shows the
440 flow curves for s/o suspensions containing PGPR 4150 or G90. At any given concentration applied
441 PGPR 4150 is more efficient in reducing yield stress than PGPR G90, which is reflected in the Casson
442 yield stress values shown in Fig. 7 and aligns with recently published Herschel-Bulkley yield stress
443 values for these PGPR products (Price et al., 2022).

444 Fig. 6B shows the flow curves for suspensions containing freeze-dried chloroplast samples P-
445 CRF, DP-CRF or B-CRF. They resemble in shape those of suspensions containing PGPR (Fig. 6A). The
446 capacity of the B-CRF material to reduce the yield was markedly lower than of P-CRF and DP-CRF. Fig.
447 6C offers a direct comparison of the yield stress reducing behaviour of the best performing chloroplast
448 material P-CRF with the better (of the two) performing PGPR 4150.

449 Using the Casson equation (Eq. 1) and flow curve data, σ_c , η_c , τ_5 and η_{40} can be calculated.
450 The dependencies of the calculated rheological parameters on emulsifier type and concentration are
451 shown in Fig. 7 (the data for η_c are provided in Appendix Fig. B.2). Comparing σ_c and τ_5 of all samples
452 reveals that PGPR 4150 is the most effective emulsifier due to its lower yield stresses values. This is
453 closely followed by PGPR G90, DP-CRF, P-CRF and B-CRF respectively. The σ_c and τ_5 values for the
454 control sample (no emulsifier) are found to be 63.5 ± 19.5 and 185.8 ± 34.2 Pa, respectively. Addition
455 of 0.1% of PGPR 4150 resulted in a decrease of σ_c and τ_5 by 93.2% (4.3 ± 2.0 Pa) and 83.7% ($30.3 \pm$
456 7.6 Pa), respectively. PGPR G90, however, reduced σ_c only by 51.8% (30.6 ± 4.1 Pa) and τ_5 by 60.2%
457 (74.0 ± 8.3 Pa).

458 Although less effective than PGPR, the three chloroplast/thylakoid materials tested (P-CRF,
459 DP-CRF and B-CRF) clearly demonstrated a strong ability to reduce the yield value of the highly
460 concentrated s/o suspension, acting as a chocolate model system. At 1.0%, DP-CRF performed slightly
461 better than P-CRF and B-CRF, reducing σ_c and τ_5 to 2.0 ± 0.3 and 26.9 ± 1.7 Pa, respectively. 1.0% P-
462 CRF and B-CRF both lead to significantly higher values of σ_c and τ_5 ; P-CRF: 5.37 ± 2.36 and $39.68 \pm$
463 6.82 Pa; B-CRF: 6.02 ± 1.56 and 40.04 ± 5.07 Pa, respectively. Further increase in the concentration of

464 any of the chloroplast/thylakoid materials (2.0% and 3.0%) resulted in a diminishing emulsifier
465 effectiveness. According to Figure 7, the σ_c data illustrates that the efficiency of chloroplast/thylakoid
466 material in aiding flowability in the chocolate model system decreased from DP-CRF to P-CRF to B-
467 CRF. This phenomenon is marked by 1.0 and 2.0% concentration of the chloroplast material. It was
468 hypothesised that the emulsifying ability of CRF material is correlated to the galactolipids content in
469 each sample. From the analysis, the galactolipids (i.e., MGDG and DGDG) concentration is highest in
470 DP and P-CRF sample with approximately 42 – 33 $\mu\text{g/g}$ DW. In B-CRF, however, the galactolipids fall to
471 about 17 $\mu\text{g/g}$ DW. This observation supports the result seen from the unidirectional and oscillatory
472 measurements.

473 The oscillatory rheology data were used to determine the tangent flow point (TFP) and the
474 cross over point (COP). As aforementioned, for samples showing modulus discontinuity, TFP and COP
475 coincided (TFP = COP). The dependency of TFP and COP on emulsifier type and concentration is shown
476 in Fig. 8 and it mirrors that of σ_c and τ_5 . The COP of the control sample (no emulsifier) was 6.6 ± 0.7
477 Pa. An addition of 0.2% PGPR 4150 resulted in the COP decreasing to 1.5 ± 0.4 Pa. This value is
478 comparable to those found for the addition of 1.0% DP-CRF (1.4 ± 0.2 Pa), P-CRF (1.6 ± 0.3 Pa) or B-
479 CRF (1.8 ± 0.2 Pa).

480 With an increase in emulsifier concentration, the flow behaviour transitioned from an elastic
481 ($G' > G''$) to viscous ($G'' > G'$) domination (Fig. 5). Progressively, the s/o suspension required less energy
482 to initiate flowing and as such, the COP gradually moved to lower oscillatory stresses. In the case of
483 0.6% PGPR 4150, the COP even moved outside the range of oscillatory shear stress values applied with
484 $G'' > G'$ throughout (Fig. 5). Conversely, the value for η_c approached 1 as shown in Appendix Fig. B.2.
485 However, the TFP could still be determined using the extrapolation method (0.10 ± 0.01 Pa).

486 Although the main purpose of formulating PGPR into confectionery products is to reduce the
487 yield stress, it concurrently reduces the apparent viscosity (Beckett, 2009). PGPR was observed to
488 reduce η_{40} of the control (15.4 ± 1.7 Pa s) to 2.6 ± 0.2 and 2.3 ± 0.3 Pa s upon addition of 0.2% PGPR

489 G90 and 4150, respectively. Similar to σ_c and τ_5 , no significant differences were observed between
490 adding 0.2% PGPR G90 and 1.0% DP-CRF material.

491

492 **3.3. Suspension Microstructure**

493 To gain insight into the interaction between the chloroplast/thylakoid materials and sugar
494 particles suspended in oil, the microstructure of a s/o suspension containing P-CRF was visualised
495 using confocal laser scanning microscopy. More precisely, 1.0% Rhodamine B-stained P-CRF (S-CRF)
496 was applied in a s/o suspension with the reduced sugar content of 50% (w/w) which benefitted image
497 quality. Rhodamine B is a protein-specific stain and targets the integral and peripheral proteins
498 embedded within the chloroplast membrane structures (outer-, inner-envelope and thylakoid
499 membranes). Since sugar and sunflower oil contain no protein, the features in Fig. 9 identify the
500 presence of proteins, which, in turn, indicates the presence of complex membrane systems. Fig. 9
501 illustrates the maximum intensity projection while Appendix Fig. C.3 provides micrographs obtained
502 at four different planes: Z = 1 - 4.

503 As seen on the micrograph of plane 1 (Z = 1) (Appendix Fig. C.3A), a large amount of membrane
504 structure surrounded the sugar particles ($d_{4,3} = 35.6 \pm 2.3 \mu\text{m}$, Appendix Fig. A.1) suspended in the
505 system. Each z-plane had a thickness difference of 0.2 – 0.5 μm and the micrographs (Appendix Fig.
506 C.3B, C and D) display the membrane structure located on the upper surface of the sugar particles.
507 Together, these micrographs show the image of protein-stained membranes material enveloping the
508 sugar particles on different planes. Overall, the confocal micrographs demonstrate the adsorption of
509 chloroplast/thylakoid membrane structures onto the sugar particles suspended in the system.
510 Rounded, bright red structures can also be observed in the micrograph, indicating freely suspended
511 fragments of S-CRF material.

512 Thylakoid membranes have been reported to stabilise oil-in-water emulsions by
513 encompassing the oil droplets and acting as barriers preventing coalescence (Rayner, Ljusberg, et al.,
514 2011). Such barrier properties (Rayner, Ljusberg, et al., 2011) offer a potential explanation for the
515 behaviour of chloroplast material in an oil-based suspension, similar to the mechanism proposed for
516 PGPR. PGPR molecules were observed to form pillow-like structures surrounding sugar particles
517 suspended in oil, acting as a barrier preventing these lipophobic particles to aggregate thus enhancing
518 the flow of the suspension (Middendorf, Juadjur, Bindrich, & Mischnick, 2015). Similarly, the presence
519 of chloroplast particulates at the surface of sugar particles may create a repulsive barrier that prevents
520 sugar particle agglomeration, resulting in the enhanced flowability revealed in this work.

521

522

523 4. Conclusion

524 Overall, it is possible, using physical methods, to prepare chloroplast membranes displaying a
525 range of disorder. Unidirectional and oscillatory measurements showed that the addition of
526 emulsifiers (PGPR [4150 & G90] & chloroplast/thylakoid materials [P-CRF, DP-CRF & B-CRF]) reduced
527 the energy required to initiate the flow of the s/o suspension. Progressive addition of chloroplast-
528 based emulsifier material resulted in the reduction of the yield stress measures (τ_5 and σ_c), apparent
529 viscosity (η_{40}), and COP and TFP values. An increase of the concentration of chloroplast/thylakoid
530 materials above 2.0% resulted in diminishing effectiveness. The ultimate effectiveness of these
531 material was comparable with 0.2% PGPR. By analysing confocal laser scanning micrographs of the
532 chloroplast/thylakoid materials there was evidence of chloroplast membranes surrounding sugar
533 particles. Assuming the membranes remained intact, as observed in TEM, then we are observing an
534 interaction between a multicomponent membrane at the surface of sugar particles. There is, however,
535 the possibility that the lipid elements of the membrane gradually partition into the oil phase. Given

536 that a commercial process to produce chloroplast material is likely to include a stage to knock out
537 endogenous enzymes to stabilise the material, it would of interest to test the impact of heat-
538 treatment on the properties of the chloroplast membranes.

539 Overall, this study introduces a simple physical method to prepare interfacial-active
540 chloroplast membrane material, without the need to perform any lipid extraction involving the use of
541 organic solvents. As confectionery formulations often involve PGPR (Mahamad, 2017; Peker et al.,
542 2013; Schantz & Rohm, 2005), these materials hold strong potential as nutrient-rich alternatives to
543 chemical and synthetic flow enhancer in chocolate manufacture.

544

545

546 **Acknowledgements**

547 The research published was conducted as a part of a PhD in Food Science at the University of
548 Nottingham. PS would like to convey their sincere gratitude toward Denise Mclean and Ian Ward for
549 their assistance in obtaining transmission electron and confocal micrographs, respectively.

550

551

552 **References**

- 553 Afoakwa, E. O. (2016). Cocoa processing technology. In *Chocolate Science and Technology* (pp. 102-
554 116).
- 555 Afoakwa, E. O., Paterson, A., & Fowler, M. (2007). Factors influencing rheological and textural
556 qualities in chocolate – a review. *Trends in Food Science & Technology*, 18(6), 290-298.
557 doi:<https://doi.org/10.1016/j.tifs.2007.02.002>
- 558 Afoakwa, E. O., Paterson, A., Fowler, M., & Vieira, J. (2009). Comparison of rheological models for
559 determining dark chocolate viscosity. *International Journal of Food Science & Technology*,
560 44(1), 162-167. doi:<https://doi.org/10.1111/j.1365-2621.2008.01710.x>
- 561 Albertsson, P. A., Kohnke, R., Emek, S. C., Mei, J., Rehfeld, J. F., Akerlund, H. E., & Erlanson-
562 Albertsson, C. (2007). Chloroplast membranes retard fat digestion and induce satiety: effect
563 of biological membranes on pancreatic lipase/co-lipase. *Biochem J*, 401(3), 727-733.
564 doi:10.1042/BJ20061463
- 565 Baker, B., Brown, B., & Ananteswaran, R. (2006). Measurement of yield stress in dark chocolate
566 using controlled stress vane method. *Journal of Texture Studies*, 37, 655-667.
567 doi:10.1111/j.1745-4603.2006.00076.x
- 568 Beckett, S. T. (2009). *The Science of Chocolate* (2nd ed.). Cambridge, United Kingdom: The Royal
569 Society of Chemistry.
- 570 Block, M. A., Dorne, A. J., Joyard, J., & Douce, R. (1983). Preparation and Characterization of
571 Membrane Fractions Enriched in Outer and Inner Envelope Membranes from Spinach
572 Chloroplasts. *The Journal of Biological Chemistry*, 258(21), 13281 - 13286.
- 573 Cahyani, A., Kurniasari, J., Nafingah, R., Rahayoe, S., Harmayani, E., & Saputro, A. D. (2019).
574 Determining casson yield value, casson viscosity and thixotropy of molten Chocolate using
575 viscometer. *IOP Conference Series: Earth and Environmental Science*, 355(1), 012041.
576 doi:10.1088/1755-1315/355/1/012041
- 577 Casson, N. (1959). *A Flow Equation for Pigment-oil Suspensions of the Printing Ink Type. Reprinted*
578 *from "Rheology of Disperse Systems."*
- 579 Chhabra, R. P. (1999). *Non-Newtonian flow in the process industries : fundamentals and engineering*
580 *applications / R.P. Chhabra and J.F. Richardson*. Oxford: Oxford : Butterworth-Heinemann.
- 581 De Graef, V., Depypere, F., Minnaert, M., & Dewettinck, K. (2011). Chocolate yield stress as
582 measured by oscillatory rheology. *Food Research International*, 44(9), 2660-2665.
583 doi:10.1016/j.foodres.2011.05.009
- 584 Dinkgreve, M., Paredes, J., Denn, M. M., & Bonn, D. (2016). On different ways of measuring “the”
585 yield stress. *Journal of Non-Newtonian Fluid Mechanics*, 238, 233-241.
586 doi:<https://doi.org/10.1016/j.jnnfm.2016.11.001>
- 587 EFSA Panel on Food Additives Nutrient Sources added to Food, Mortensen, A., Aguilar, F., Crebelli,
588 R., Di Domenico, A., Dusemund, B., . . . Lambré, C. (2017). Re-evaluation of polyglycerol
589 polyricinoleate (E 476) as a food additive. *EFSA Journal*, 15(3), e04743.
590 doi:<https://doi.org/10.2903/j.efsa.2017.4743>

- 591 Eischen, J.-C., & Windhab, E. J. (2002). Viscosity of Cocoa and Chocolate Products. *Applied Rheology*,
592 12(1), 32-34. doi:doi:10.1515/arh-2002-0020
- 593 Gedi, M. A., Briars, R., Yuseli, F., Zainol, N., Darwish, R., Salter, A. M., & Gray, D. A. (2017).
594 Component analysis of nutritionally rich chloroplasts: recovery from conventional and
595 unconventional green plant species. *Journal of Food Science and Technology*, 54(9), 2746-
596 2757. doi:10.1007/s13197-017-2711-8
- 597 Gedi, M. A., Magee, K. J., Darwish, R., Eakpetch, P., Young, I., & Gray, D. A. (2019). Impact of the
598 partial replacement of fish meal with a chloroplast rich fraction on the growth and selected
599 nutrient profile of zebrafish (*Danio rerio*). *Food Funct*, 10(2), 733-745.
600 doi:10.1039/c8fo02109k
- 601 Kumbár, V., Nedomová, Š., Ondrušíková, S., & Polcar, A. (2018). Rheological behaviour of chocolate
602 at different temperatures. *Potravinárstvo Slovak Journal of Food Sciences*, 12, 123-128.
603 doi:10.5219/876
- 604 Lichtenthaler, H., K., Buschmann, C. (2001). Chlorophylls and Carotenoids: Measurement and
605 Characterization by UV-Vis Spectroscopy *Current Protocols in Food Analytical Chemistry* 1(1),
606 F4.3.1 - F4.3.8. doi: <https://doi.org/10.1002/0471142913.faf0403s01>
- 607 Mahamad, N. J. (2017). *Dark Chocolate: Understanding The Impact of Limonene on the*
608 *Crystallization Properties and Application of Green Leaf Lipid Extract as a Flow Enhancer*
609 (PhD). University of Nottingham
- 610 Malvern Instruments Limited. (2012). *Understanding Yield Stress Measurements*. Retrieved from
- 611 Manasi, I., Arnold, T., Cooper, J. F. K., Van Damme, I., Dong, C., Saerbeck, T., . . . Titmuss, S. (2019).
612 Planar sucrose substrates for investigating interfaces found in molten chocolate. *Food*
613 *Structure*, 22, 100128. doi:10.1016/j.foostr.2019.100128
- 614 Middendorf, D., Juadjur, A., Bindrich, U., & Mischnick, P. (2015). AFM approach to study the function
615 of PGPR's emulsifying properties in cocoa butter based suspensions. *Food Structure*, 4, 16-
616 26. doi:<https://doi.org/10.1016/j.foostr.2014.11.003>
- 617 Food Additives in Europe 2000 - Status of safety assessments of food additives presently permitted
618 in the EU (2002).
- 619 Mohamad, N. J., Gray, D., & Wolf, B. (2020). Spinach leaf and chloroplast lipid: A natural rheology
620 modifier for chocolate? *Food Research International*, 133, 109193.
621 doi:<https://doi.org/10.1016/j.foodres.2020.109193>
- 622 Osborn, S. (2015). 12 - Labelling relating to natural ingredients and additives. In P. Berryman (Ed.),
623 *Advances in Food and Beverage Labelling* (pp. 207-221). Oxford: Woodhead Publishing.
- 624 Ostbring, K., Sjöholm, I., Sorenson, H., Ekholm, A., Erlanson-Albertsson, C., & Rayner, M. (2018).
625 Characteristics and functionality of appetite-reducing thylakoid powders produced by three
626 different drying processes. *J Sci Food Agric*, 98(4), 1554-1565. doi:10.1002/jsfa.8627
- 627 Peker, B. B., Suna, S., Tamer, C. E., & Copur, O. U. (2013). The Effect of Lecithin and Polyglycerol
628 Polyricinoleate (PGPR) on Quality of Milk, Bitter and White Chocolates *Journal of Agricultural*
629 *Faculty of Uludag University*, 1-16.

630 Pratumwal, Y., Limtrakarn, W., Muengtaweepongsa, S., Phakdeesan, P., Duangburong, S., Eiamaram,
631 P., & Intharakham, K. (2017). Whole blood viscosity modeling using power law, Casson, and
632 Carreau Yasuda models integrated with image scanning U-tube viscometer technique.
633 *Songklanakarin Journal of Science and Technology*, 39, 625-631. doi:10.14456/sjst-
634 psu.2017.77

635 Price, R., Gray, D., Watson, N., Vieira, J., & Wolf, B. (2022). Linking the yield stress functionality of
636 polyglycerol polyricinoleate in a highly filled suspension to its molecular properties. *LWT*,
637 165, 113704. doi:https://doi.org/10.1016/j.lwt.2022.113704

638 Quest International. (1997). *Summary of Legislative Approvals for Polyglycerol Polyricinoleate (PGPR)*
639 *Admul WOL TM*. Retrieved from

640 Rao, M. A. (2014). Flow and Functional Models for Rheological Properties of Fluid Foods. 27-61.
641 doi:10.1007/978-1-4614-9230-6_2

642 Rayner, M., Emek, S. C., Gustafssona, K., Albertsson, C. E., & Albertsson, P.-Å. (2011). A novel
643 emulsifier from spinach with appetite regulation abilities. *Procedia Food Science*, 1, 1431-
644 1438. doi:10.1016/j.profoo.2011.09.212

645 Rayner, M., Ljusberg, H., Emek, S. C., Sellman, E., Erlanson-Albertsson, C., & Albertsson, P.-Å. (2011).
646 Chloroplast thylakoid membrane-stabilised emulsions. *Journal of the Science of Food and*
647 *Agriculture*, 91(2), 315-321. doi:10.1002/jsfa.4187

648 Schantz, B., & Rohm, H. (2005). Influence of lecithin–PGPR blends on the rheological properties of
649 chocolate. *LWT - Food Science and Technology*, 38(1), 41-45. doi:10.1016/j.lwt.2004.03.014

650 Schindelin, J., Arganda-Carreras, I., Frise, E., Kaynig, V., Longair, M., Pietzsch, T., . . . Cardona, A.
651 (2012). Fiji: an open-source platform for biological-image analysis. *Nature Methods*, 9(7),
652 676-682. doi:10.1038/nmeth.2019

653 Servais, C., Ranc, H., & Roberts, I. D. (2003). DETERMINATION OF CHOCOLATE VISCOSITY. *Journal of*
654 *Texture Studies*, 34(5-6), 467-497. doi:https://doi.org/10.1111/j.1745-4603.2003.tb01077.x

655 Shafi, F., Reshi, M., Aiman, & Bashir, I. (2018). Chocolate Processing *International Journal of*
656 *Advanced Biological Research* 8(3), 408 - 419.

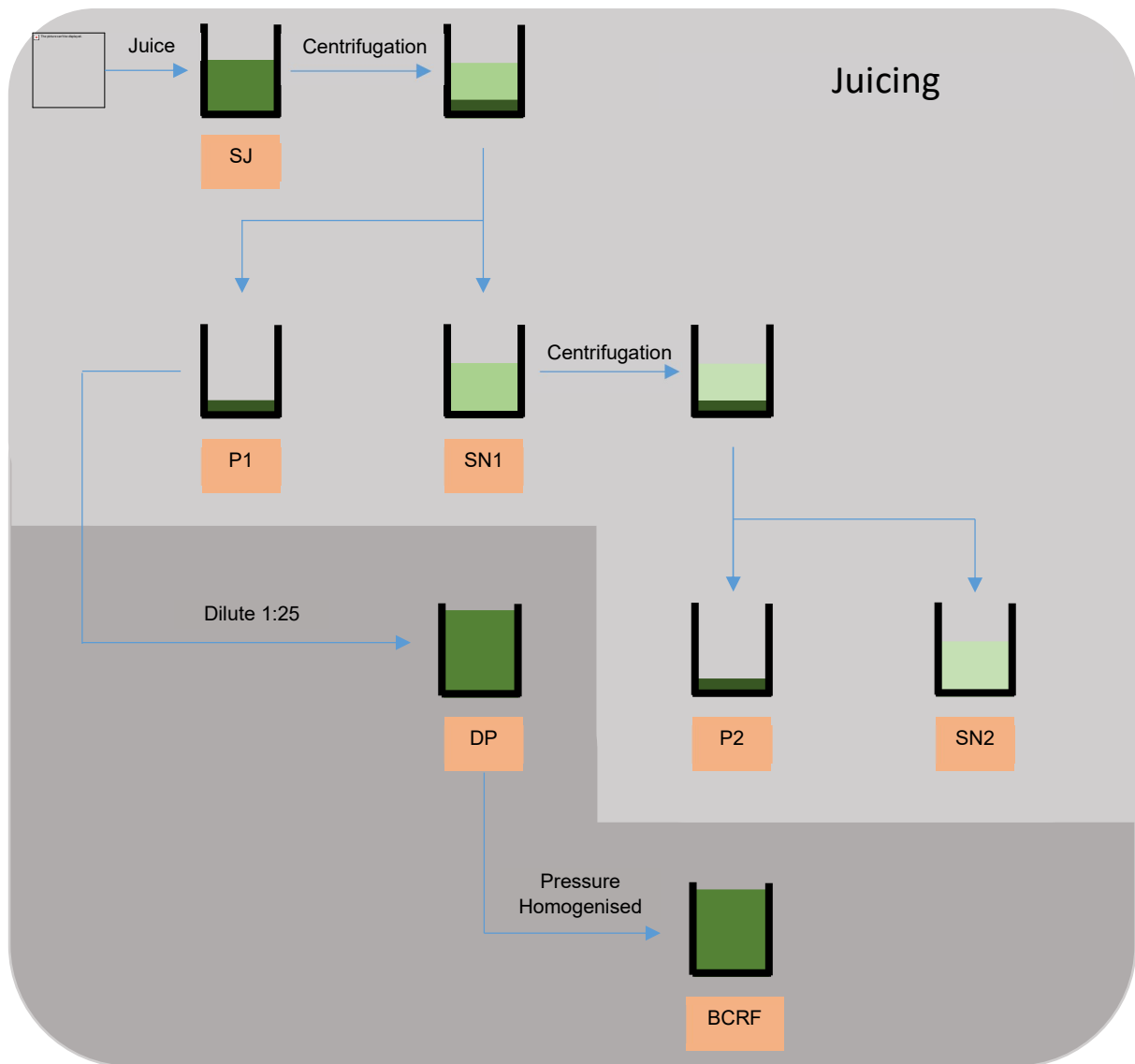
657 Shimoni, E., Rav-Hon, O., Ohad, I., Brumfeld, V., & Reich, Z. (2005). Three-dimensional organization
658 of higher-plant chloroplast thylakoid membranes revealed by electron tomography. *Plant*
659 *Cell*, 17(9), 2580-2586. doi:10.1105/tpc.105.035030

660 Sözeri Atik, D., Bölük, E., Toker, O. S., Palabiyik, I., & Konar, N. (2020). Investigating the effects of
661 Lecithin-PGPR mixture on physical properties of milk chocolate. *LWT*, 129, 109548.
662 doi:https://doi.org/10.1016/j.lwt.2020.109548

663 Staehelin, L. A. (1986). *Chloroplast Structure and Supramolecular Organization of Photosynthesis*
664 *Membranes* (Vol. 19). Germany Springer-Verlag.

665 Syamila, M., Gedi, M. A., Briars, R., Ayed, C., & Gray, D. A. (2019). Effect of temperature, oxygen and
666 light on the degradation of beta-carotene, lutein and alpha-tocopherol in spray-dried
667 spinach juice powder during storage. *Food Chem*, 284, 188-197.
668 doi:10.1016/j.foodchem.2019.01.055

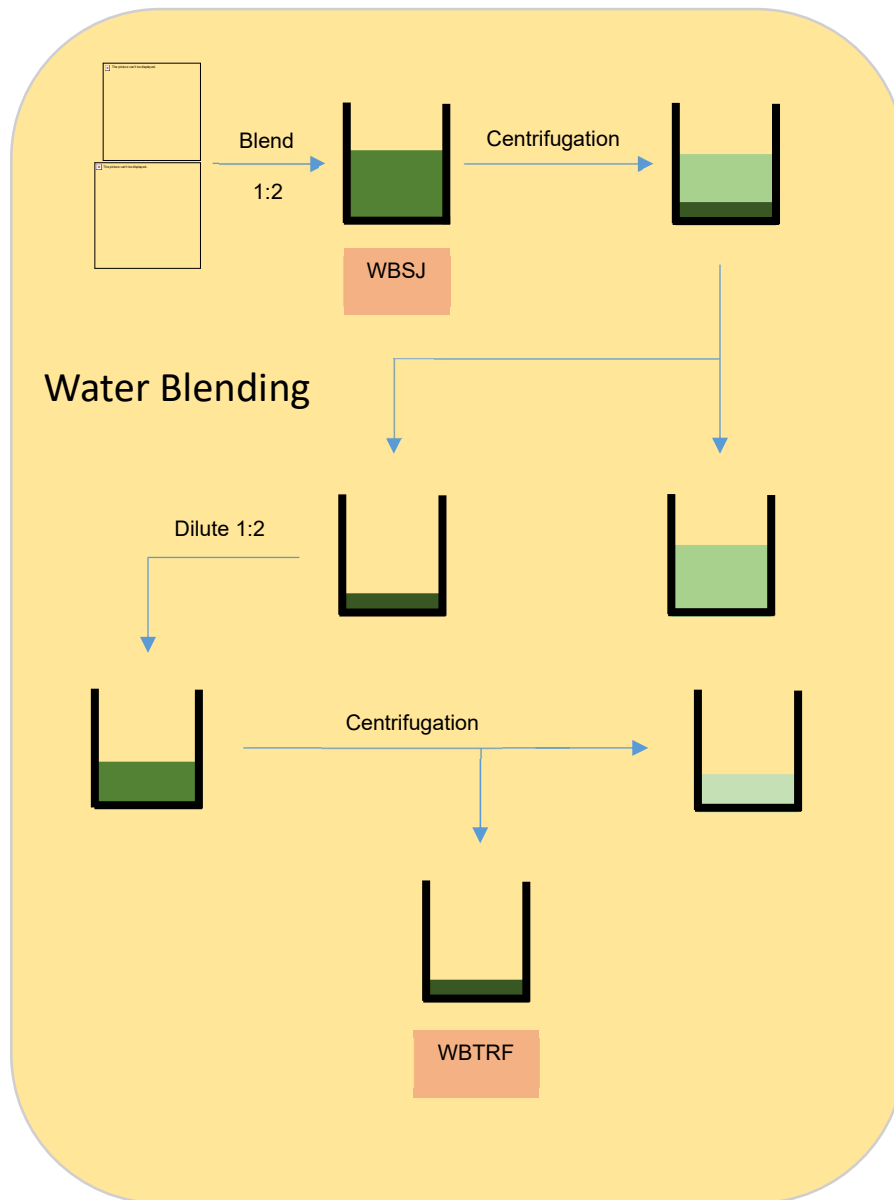
- 669 Tenorio, A. T., de Jong, E. W., Nikiforidis, C. V., Boom, R. M., & van der Goot, A. J. (2017). Interfacial
670 properties and emulsification performance of thylakoid membrane fragments. *Soft Matter*,
671 13(3), 608-618. doi:10.1039/c6sm02195f
- 672 Torcello-Gomez, A., Gedi, M. A., Ibbett, R., Nawaz Husain, K., Briars, R., & Gray, D. (2019).
673 Chloroplast-rich material from the physical fractionation of pea vine (*Pisum sativum*)
674 postharvest field residue (Haulm). *Food Chem*, 272, 18-25.
675 doi:10.1016/j.foodchem.2018.08.018
- 676 Wattanakul, J., Sahaka Mahaman Salah, M. B., Amara Ep Douzi, S., Syamila, M., Gontero, B., Carrière,
677 F., & Gray, D. (2019). In vitro digestion of galactolipids from chloroplast-rich fraction (CRF) of
678 postharvest, pea vine field residue (haulm) and spinach leaves. *Food & Function*, 10.
679 doi:10.1039/C9FO01867K
- 680 Wattanakul, J., Syamila, M., Briars, R., Ayed, C., Price, R., Darwish, R., . . . Gray, D. A. (2021). Effect of
681 steam sterilisation on lipophilic nutrient stability in a chloroplast-rich fraction (CRF)
682 recovered from postharvest, pea vine field residue (haulm). *Food Chem*, 334, 127589.
683 doi:10.1016/j.foodchem.2020.127589
- 684 Wattanakul, J., Syamila, M., Darwish, R., Gedi, M. A., Sutcharit, P., Chi, C., . . . Gray, D. A. (2022).
685 Bioaccessibility of essential lipophilic nutrients in a chloroplast-rich fraction (CRF) from
686 agricultural green waste during simulated human gastrointestinal tract digestion. *Food &*
687 *Function*, 13(9), 5365-5380. doi:10.1039/D2FO00604A
- 688 Wayne, R. (2019). *Chloroplasts*: Elsevier Science Publishing Co Inc.
- 689 Wilson, R., Van Schie, B. J., & Howes, D. (1998). Overview of the preparation, use and biological
690 studies on polyglycerol polyricinoleate (PGPR). *Food Chem Toxicol*, 36(9-10), 711-718.
691 doi:10.1016/s0278-6915(98)00057-x
- 692 Windhab, E. (1993). Bericht: IV. *Tagung Lebensmittel rheologie detmold*.
- 693 Wolf, F., Koehler, K., & Schuchmann, H. P. (2013). Stabilization of Water Droplets in Oil with PGPR for
694 Use in Oral and Dermal Applications. *Journal of Food Process Engineering*, 36(3), 276-283.
695 doi:https://doi.org/10.1111/j.1745-4530.2012.00688.x
- 696



698

699 **Figure 1:** Simplified flow chart for the preparation of largely intact chloroplast (P1 and P2), untangled
700 chloroplast membrane (diluted pellet, DP) and burst chloroplast-rich fraction (BCRF) via juicing from
701 spinach leaves. SJ: spinach juice, P1 and SN1: pellet and supernatant respectively from centrifuged SJ,
702 P2 and SN2: pellet and supernatant respectively from centrifuged SN1.

703



704

705

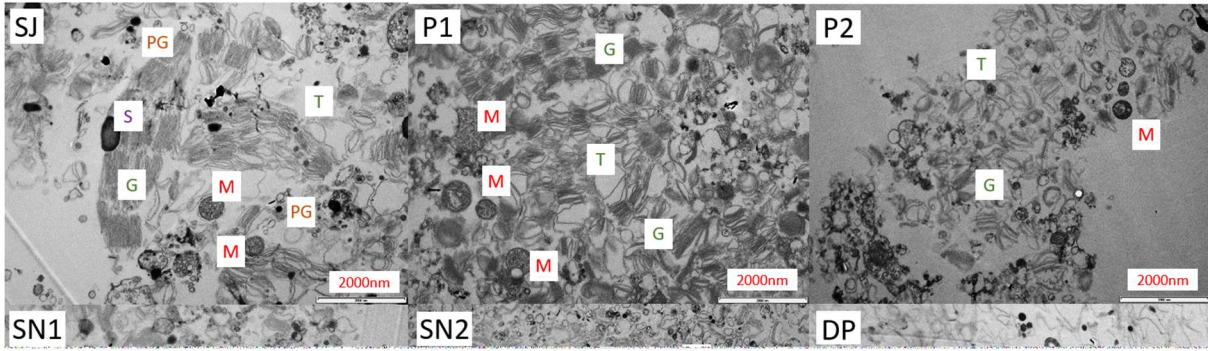
706 **Figure 2:** Simplified flow chart for the preparation of water-blended thylakoid-rich fraction (WBTRF)

707 from water-blended spinach juice (WBSJ).

708

709

710



711

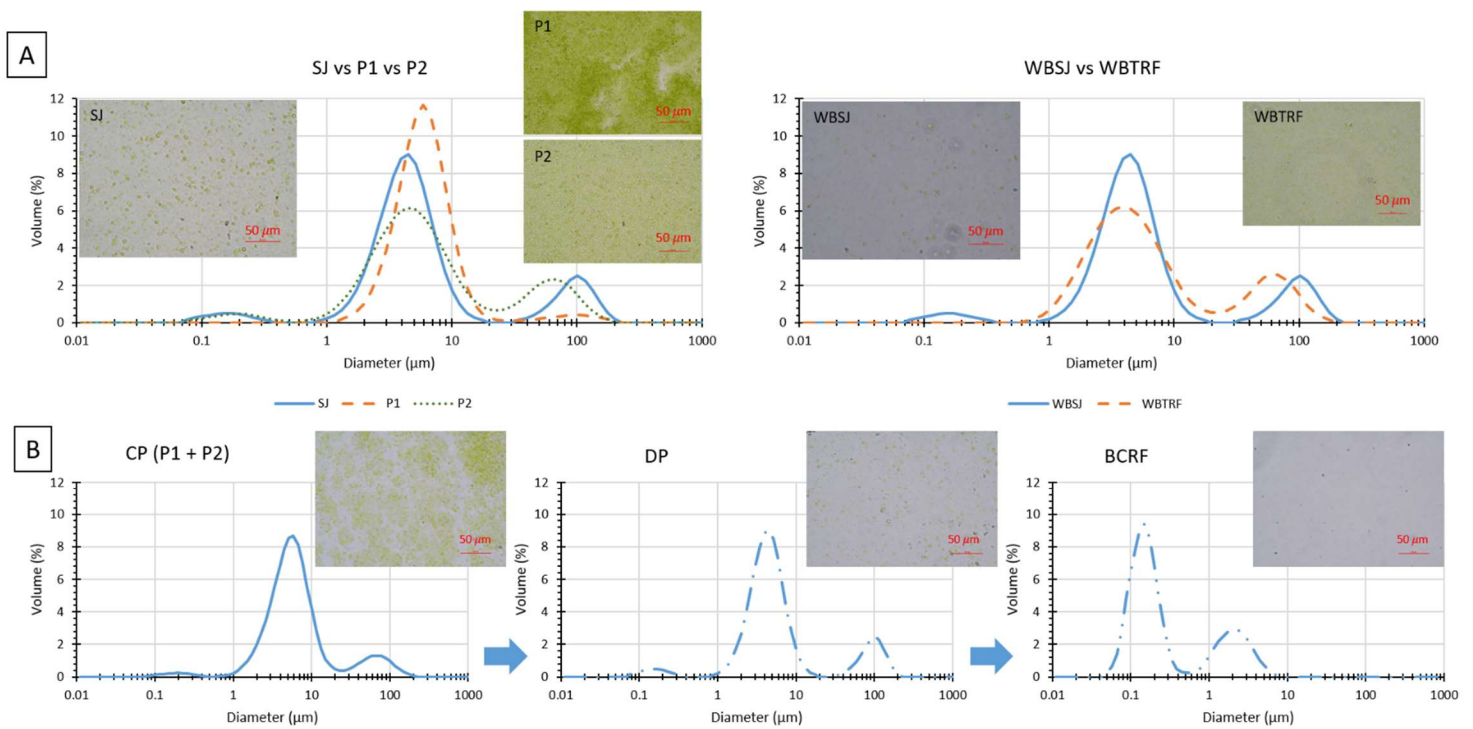
712 **Figure 3:** Transmitted electron micrographs of chloroplast materials taken at X9900 magnification. The
 713 samples are as follow: spinach juice (SJ), pellet 1 (P1), pellet 2 (P2), supernatant 1 (SN1), supernatant
 714 2 (SN2), dilute spinach juice (DP), burst-chloroplast-rich fraction (BCRF), water blended spinach juice
 715 (WBSJ) and water blended thylakoid-rich fraction (WBTRF). Structures labelled include: Starch (S),
 716 Mitochondria (M), Thylakoid (T), Grana (G), and Plastoglobule (PG). All scale bars correspond to 2000
 717 nm.

718

719

720

721

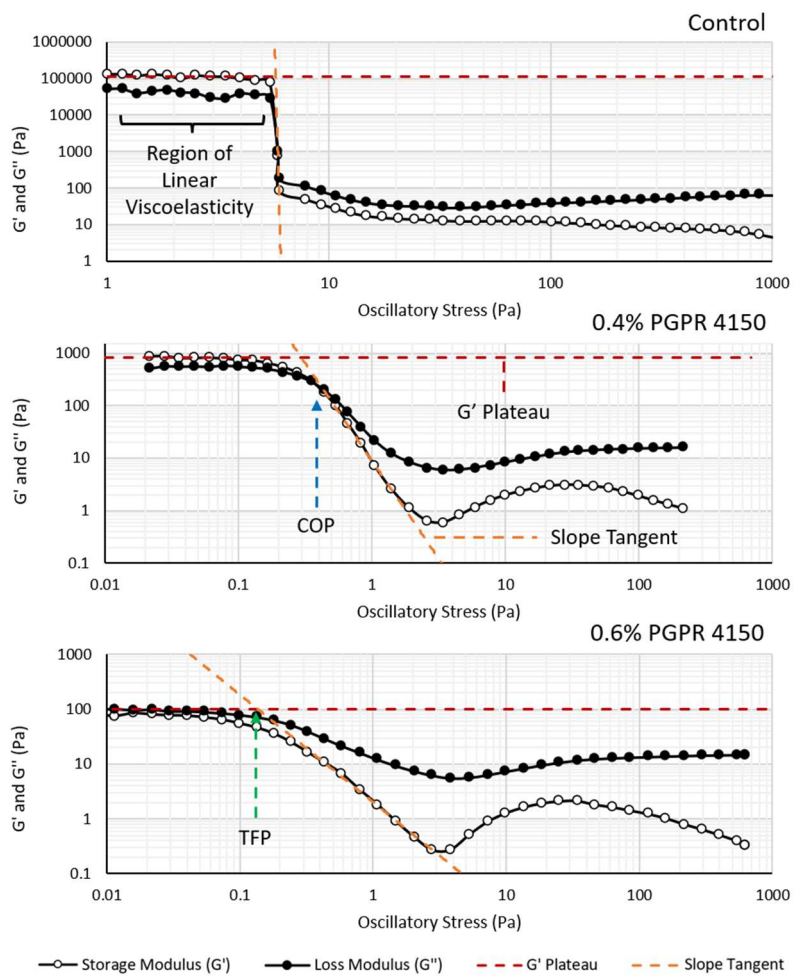


723

724 **Figure 4:** Particle size distribution and corresponding transmission light micrographs of
 725 chloroplast/thylakoid samples prepared from juicing and blending method. (A) The left-hand panel
 726 shows the effect of sequential centrifugation on the particle size profile of spinach juice sample
 727 obtained from extrusion (SJ) and the right-hand panel the water-blended spinach juice (WBSJ)
 728 (Smooth line). The pellet samples from juicing method are pellet 1 (P1) (Dashed line) and pellet 2 (P2)
 729 (Dotted line), while water blended thylakoid-rich fraction (WBTRF) (Dashed line) represents the pellet
 730 sample after centrifugation of the sample obtained from WB-method. In (B), the effect of dilution and
 731 pressure homogenization on the overall pellet sample (P1 + P2) particle size is illustrated. All
 732 transmission light micrographs were obtained at 400X total magnification, and all scale bars
 733 correspond to 50 μm.

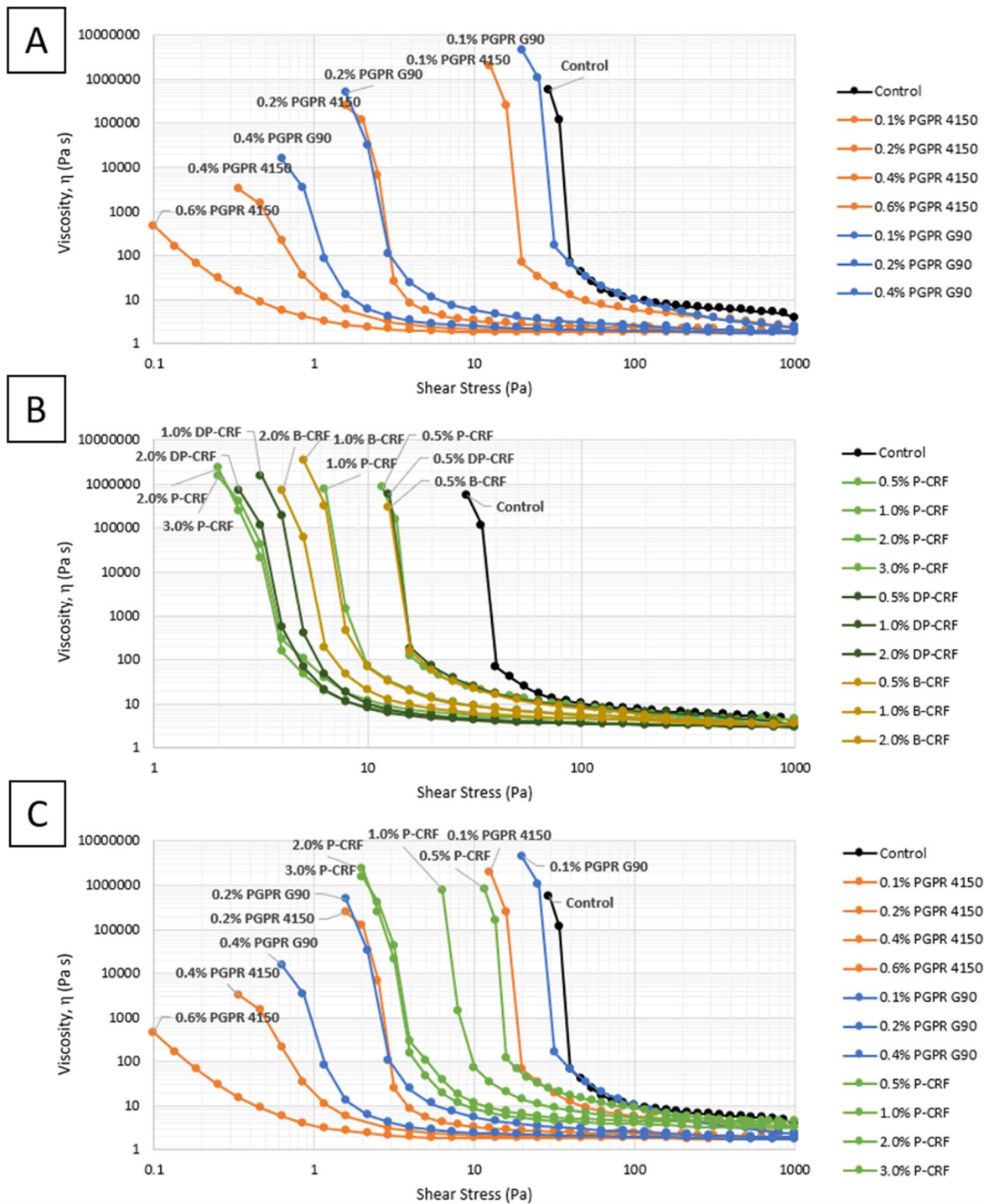
734

735



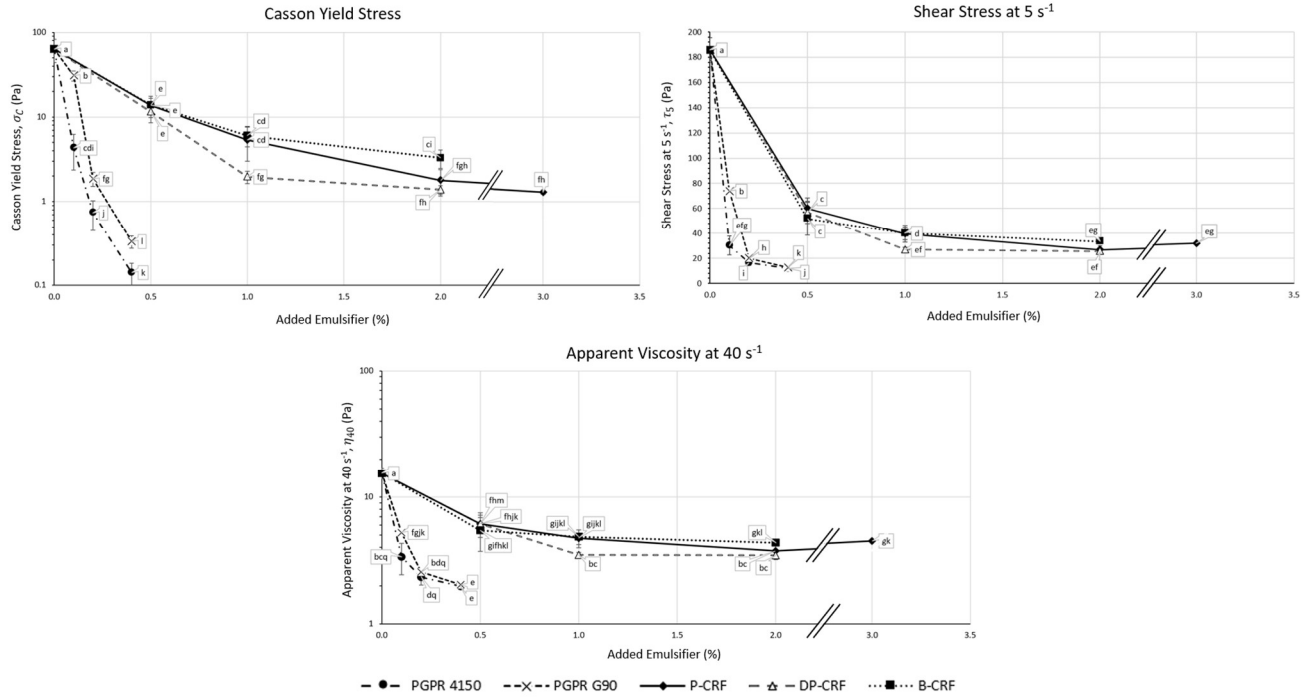
737

738 **Figure 5:** Determination of tangent flow point (TFP) from oscillatory measurements: Control (A), 0.4%
 739 PGPR 4150 (B) and 0.6% PGPR 4150 (C). The red and yellow dashed lines represent the tangent lines
 740 plotted using data points from the region of linear viscoelasticity (i.e., G' Plateau) and the decaying
 741 portion of G' data (i.e., slope tangent), respectively. The cross over between the G' and G'' lines is
 742 referred to as the cross over point (COP) while the cross between the tangent lines, the TFP. At 0%
 743 PGPR (control), a discontinuity point is observed. For the stress values below the discontinuity point,
 744 the sample display an elasticity dominated behaviour ($G' > G''$) while for the stress values above the
 745 discontinuity point the sample display a viscosity dominated behaviour ($G'' > G'$). In this case, the TFP
 746 and cross over point (COP) coincided.



747

748 **Figure 6:** Flow curves obtained from unidirectional measurements following a ramp-down protocol
 749 (1,000 Pa to 0.01 Pa). (A) Suspensions containing PGPR 4150 or PGPR G90, and control. (B) Suspensions
 750 containing any of the three chloroplast/thylakoid materials P-CRF, DP-CRF or B-CRF, and control. (C)
 751 Suspensions containing PGPR 4150 or PGPR G90 or P-CRF material, and control.



752

753 **Figure 7:** A reduction in Casson yield stress (σ_C), shear stress at 5 s^{-1} (τ_5) and apparent viscosity (η_{40})
 754 obtained from unidirectional experiments. The statistical differences are denoted by lowercase
 755 letters.

756

757

758

759

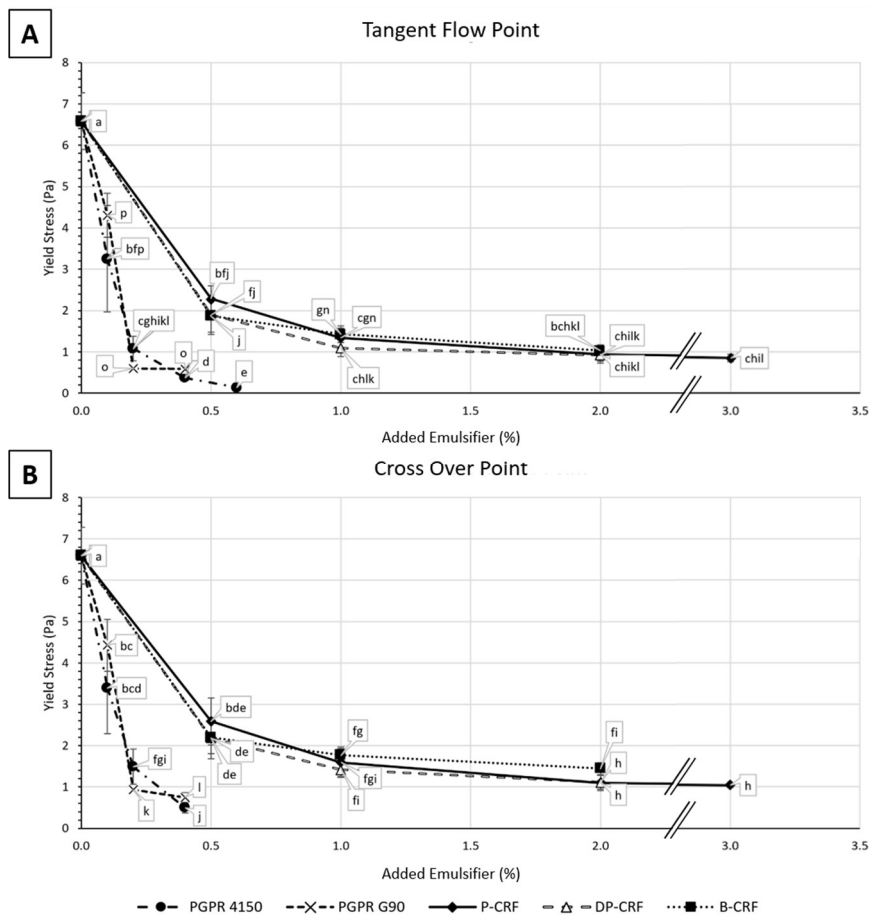
760

761

762

763

764

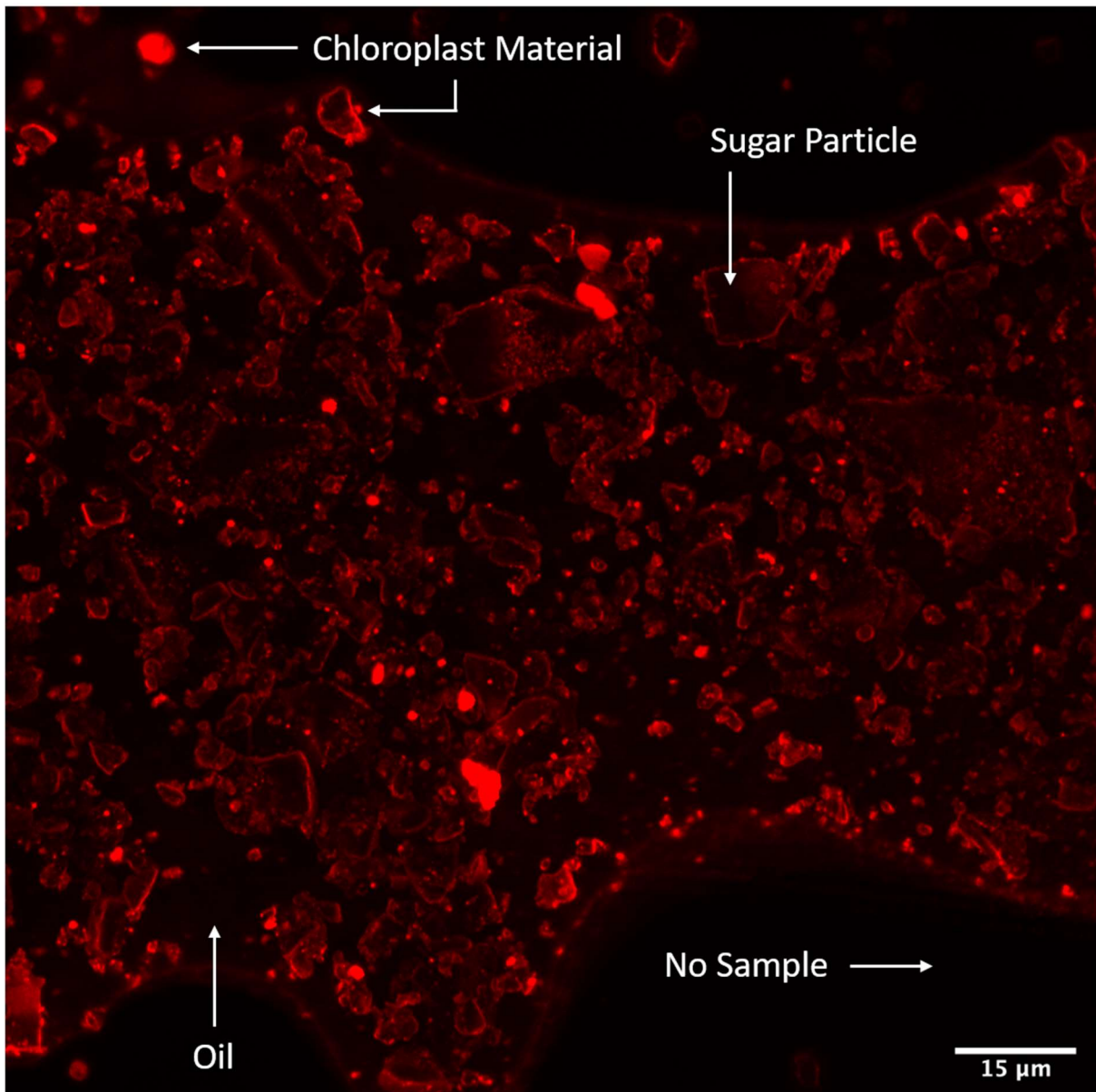


765

766 **Figure 8:** A reduction in Tangent Flow Point (TFP) and Cross Over Point (COP) obtained from oscillatory
 767 rheological experiments. The statistical analysis for all data is represented with lowercase letters. For
 768 0.6% PGPR 4150, the sample displayed a viscosity dominated behaviour ($G'' > G'$) throughout the
 769 tested range. As such, 0.6% PGPR 4150 do not possess a COP but the value for TFP can be determined
 770 via extrapolation.

771

772



773

774 **Figure 9:** Maximum intensity projection confocal Micrographs of 1.0% S-CRF (Rhodamine B-stained
 775 pellet chloroplast-rich fraction) in 50% s/o suspension at X63 objective lens (Z stacks = 20). Under 561
 776 nm lamp, structures appear in red indicate the protein-stained chloroplast material (Rhodamine B,
 777 λ_{ext} : 553 nm, λ_{emi} : 627 nm). Black region is area with no sample, while the lighter red region indicates
 778 the oil phase. Scale bar represents 15 μ m.

779

780

